

First Example of a Nonanuclear Silver Sulfate Hybrid Cluster: Green Approach for Synthesis of Lewis Acid Catalyst

Avijit Kumar Paul,* Kumari Naveen, Nikhil Kumar, Rajendiran Kanagaraj, V. M. Vidya and Tanmay Rom

Department of Chemistry, National Institute of Technology Kurukshetra, Kurukshetra-136119,
Haryana, India.

E-mail: apaul@nitkkr.ac.in

ELECTRONIC SUPPORTING INFORMATION

* Dr. Avijit Kumar Paul
Department of Chemistry
National Institute of Technology Kurukshetra
Kurukshetra-136119, Haryana, India.
E-mail: apaul@nitkkr.ac.in

Supporting information for this article is given via a link at the end of the document.

Procedure for synthesis of compound I and catalytic reactions

Solvothermal Condition:

The resulting reaction mixture with the composition, $1\text{Ag}_2\text{SO}_4 : 1\text{C}_3\text{H}_6\text{N}_6 : 85\text{EtOH} : 389\text{H}_2\text{O}$ was sealed in a 23 mL PTFE lined autoclave and heated at 125 °C for 3 days under autogeneous pressure. The final product, containing very few colorless rectangular crystals, was filtered, washed with deionized water under vacuum and dried at ambient conditions (yield ~ 70% based on Ag).

Mechanochemical Strategy:

For synthesis of pure powdered compound I, a mixture of Ag_2SO_4 (0.31g, 1mM) and melamine (0.095g, 0.75mM) was taken in a mortar-pestle. The mixture was ground for 2 hours to homogenize properly. Afterwards few drops of EtOH were added at the time of grinding for improvement of homogeneity. The finely ground mixture was kept inside the oven at 125 °C for 3 days. The pure white powdered compound was characterized by PXRD which shows the purity of the compound (Fig. S1).

Catalytic Reactions:

In a typical experiment for cyanosilylation reaction, powdered catalyst was suspended in 100 ml round bottom flask with the CH_2Cl_2 solvent and N-benzilidine aniline (see Supporting Information). Trimethylsilyl cyanide was added to it at 0 °C and the overall mixture was stirred for 2 h in N_2 atmosphere. The product was filtered through Millipore membrane filter papers to remove the catalyst particles.

For ketal formation, we used three different ketones i.e. acetone, 2-butanone and 3-pentanone. Typically, 0.02 mmol portion of the silver sulfate catalyst, 16 mmol of ketone, and 16 mmol of ethylene glycol were introduced into 10 mL of toluene, the latter was used as the solvent for a ketal formation reaction. The reaction was refluxed at 60 °C for 10 h. After completion of the reaction, the catalyst was isolated by filtration and reused on subsequent reactions without further treatment. All product yields were determined by ^1H NMR spectra (See below).

For esterification reaction, 0.02 mmol catalyst, 16 mmol of acetic acid, and 16 mmol of ethanol were introduced into 10 mL of toluene for this catalytic reaction. The esterification reaction was also conducted for an additional 6 h to improve the percentage of yield. The unsatisfactory result proves the effectiveness of catalyst.

Table 1. Single crystal data and structure refinement parameters for **I**.

A suitable colorless rectangular single crystal was carefully selected under a polarizing microscope and glued to a thin glass fiber with a cyanoacrylate (superglue) adhesive. The single-crystal data were collected on a Bruker AXS smart Apex CCD diffractometer at 293(2) K. The X-ray generator was operated at 50 kV and 35 mA using Mo K α ($\lambda = 0.71073$ Å) radiation. The data were reduced using SAINTPLUS,¹ and an empirical absorption correction was applied using the SADABS program.² The structure was solved and refined using SHELXL97³ present in the WinGx suit of programs (Version 1.63.04a).⁴ Hydrogen atoms attached to melamine units could not be located. The final refinement included atomic positions for all of the atoms and isotropic thermal parameters for all the non-hydrogen atoms. Full-matrix least-squares refinement against F^2 was carried out using the WinGx package of programs. Details of the structure solution and final refinements for all the structures are given in Table.

The crystallographic data can be found in CCDC: charge from Crystallographic Data

Structural parameter	I
Empirical formula	Ag ₈ S ₄ O ₁₆ C ₉ N ₁₈ H ₁₈
Formula weight	1625.47
Crystal system	Triclinic
Space group	<i>P</i> -1
<i>a</i> (Å)	9.7628(2)
<i>b</i> (Å)	10.1956(4)
<i>c</i> (Å)	16.5042(5)
α (°)	87.646(3)
β (°)	76.718(2)
γ (°)	86.763(3)
<i>V</i> (Å ³)	1595.63(9)
<i>Z</i>	2
T/K	293
ρ (g/cm ⁻³)	3.346
μ (mm ⁻¹)	5.162
λ (Mo K α /Å)	0.71073
θ range (°)	2.73 to 50.00
R _{int}	0.0449
R indexes [<i>I</i> > 2 σ (<i>I</i>)]	R ₁ = 0.0933 wR ₂ = 0.2577
R indexes (all data)	R ₁ = 0.1022 wR ₂ = 0.2620

data for compounds No. 1496359 by free of Cambridge Center (CCDC) via

$R_1 = \frac{\sum |F_o| - |F_c|}{\sum |F_o|}$; $wR_2 = \left\{ \frac{\sum [w (F_o^2 - F_c^2)]}{\sum [w (F_o^2)^2]} \right\}^{1/2}$. $w = 1/[\rho^2(F_o)^2 + (aP)^2 + bP]$. $P = [\max(F_o^2, O) + 2(F_c^2)/3]$ for **I**, $a = 0.1231$ $b = 125.4206$

Ref.

1. SMART (V 5.628), SAINT (V 6.45a), XPREP, SHELXTL, Bruker AXS Inc. Madison, Wisconsin, USA, 2004.
2. Sheldrick, G. M. *Siemens Area Detector Absorption Correction Program*, University of Göttingen, Göttingen, Germany, 1994.
3. G. M. Sheldrick, *SHELXL-97 Program for Crystal Structure Solution and Refinement*, University of Göttingen, Göttingen, Germany, 1997.
4. J. L. Farrugia, *J. Appl. Crystallogr.* 1999, **32**, 837.

Table 2. Selected bond distances in Silver Sulfate compound $[\text{Ag}_8(\text{SO}_4)_4(\text{C}_3\text{H}_6\text{N}_9)_3] \text{I}$.

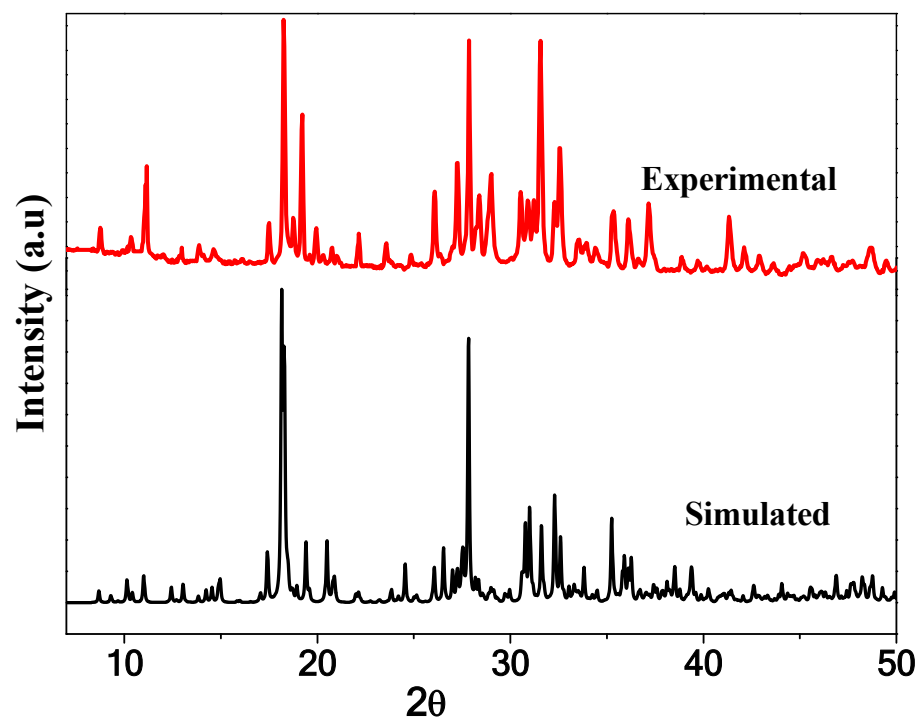
Bond	Distance (Å)	Bond	Distance (Å)	Bond	Distance (Å)
Ag(1)-O(4)	2.386(16)	Ag(5)-O(11)	2.296(19)	S(1)-O(1)	1.468(15)
Ag(1)-O(6)	2.458(13)	Ag(5)-O(14)	2.33(2)	S(1)-O(3)	1.478(14)
Ag(1)-O(6)	2.496(14)	Ag(5)-N(2)	2.234(14)	S(1)-O(4)	1.466(16)
Ag(1)-N(3)	2.276(14)	Ag(5)-Ag(6)	3.179(4)	S(1)-O(16)	1.498(13)
Ag(2)-O(3)	2.262(2)	Ag(6)-O(5)	2.509(17)	S(2)-O(2)	1.464(13)
Ag(2)-O(5)	2.58(2)	Ag(6)-N(4)	2.315(15)	S(2)-O(5)	1.472(18)
Ag(2)-O(15)	2.47(2)	Ag(6)-Ag(6)	2.819(7)	S(2)-O(11)	1.48(2)
Ag(2)-N(10)	2.227(15)	Ag(7)-O(9)	2.358(18)	S(2)-O(12)	1.464(16)
Ag(2)-Ag(4)	3.315(2)	Ag(7)-O(10)	2.44(2)	S(3)-O(6)	1.457(14)
Ag(3)-N(6)	2.237(14)	Ag(7)-O(12)	2.298(16)	S(3)-O(7)	1.472(16)
Ag(3)-O(2)	2.355(14)	Ag(7)-N(7)	2.216(15)	S(3)-O(8)	1.487(14)
Ag(3)-O(13)	2.44(3)	Ag(8)-N(14)	2.222(15)	S(3)-O(9)	1.456(18)
Ag(3)-O(2)	2.559(13)	Ag(8)-O(16)	2.246(14)	S(4)-O(10)	1.442(19)
Ag(4)-O(1)	2.335(15)	Ag(8)-O(8)	2.414(15)	S(4)-O(13)	1.40(3)
Ag(4)-O(9)	2.56(2)	Ag(8)-Ag(9)	3.061(5)	S(4)-O(14)	1.51(2)
Ag(4)-O(10)	2.376(16)	Ag(9)-O(1)	2.567(16)	S(4)-O(15)	1.48(2)
Ag(4)-N(13)	2.230(16)	Ag(9)-N(9)	2.305(15)		
		Ag(9)-Ag(9)	2.389(7)		

Table 3. Earlier reported few silver-clusters and their applications.

Different structure	Structure novelty and applications
$[\text{Ag}_{16}(\text{SO}_4)_8][\text{Ag}_4(\text{SO}_4)_2]$ and $[\text{Ag}_{10}(\text{SO}_4)_5]$. ¹	The complex containing $[\text{Ag}_{16}(\text{SO}_4)_8][\text{Ag}_4(\text{SO}_4)_2]$ subunits exhibits two kinds of cages assembled with 12-connected $[\text{Ag}_{16}(\text{SO}_4)_8]$ units and 8-connected $[\text{Ag}_4(\text{SO}_4)_2]$ units. Second complex features 14-connected $[\text{Ag}_{10}(\text{SO}_4)_5]$ clusters with highest connectivity Ag(I) cluster SBU reported till the date.
$[\text{Ag}_4(\text{H}_2\text{bpz})_4(\text{SO}_4)_2] \cdot \text{H}_2\text{O}$ (1), $[\text{Ag}_2(\text{H}_2\text{bpz})_2(\text{SO}_4)] \cdot 3\text{H}_2\text{O}$ (2), and $[\text{Ag}_3(\text{H}_2\text{bpz})_4](\text{SO}_4)_{2/3}(\text{OH})_{5/3} \cdot 4\text{H}_2\text{O}$ (3) ²	Complexes 1-3 have diverse coordination environments of Ag (I) centers and different interplanar dihedral angles of H_2bpz in them. The cationic frameworks and small-sized pores decorated by coordinately unsaturated Ag (I) centers, while methyl and -NH groups of H_2bpz offer highly polar pores in 3. The solid-state luminescence with different emission energies observed along with high heat of sorption for CO_2 and high CO_2/N_2 selectivity. In addition, 3 displays outstanding resistance toward water.
$[\text{Ag}_8(\text{SO}_4)_2]$ ³	Octanuclear silver (I) cluster with two-dimensional layer structure. The results show that the argentophilic interactions do great influence on the photoluminescent properties.
$[\text{Ag}_2(\text{H}_2\text{btec})(\text{H}_2\text{O})]$ (1), $[\text{Ag}_3(\text{Hbtec})]$ (2), and $[\text{Ag}_4(\text{btec})]$ (3) ⁴	The tetramer units show that the argentophilic interactions with greater influence on the photoluminescent properties. These materials can regulate the sustained release of silver ions leading to excellent antibacterial activities towards both Gram-negative bacteria, <i>E. coli</i> and Gram-positive bacteria, <i>S. aureus</i> .
$\text{Ag}_2(\text{DPA})$ ⁵	Silver lining: a string of argentophilic Ag (I) ions and straddling large aromatic pyrazolate linkers form a 2D network to impact significantly the photoluminescence and optical absorption properties.
$[\text{Ag}_8(\text{ADC})_4]_n$ ⁶	Octanuclear silver (I) cluster compound based on 1,3-adamantanedicarboxylic acid. Compound exhibits significant Ag-Ag interactions to form 2D infinite silver layer with multiple unsaturated Ag atoms. Photoluminescence studies show the compound can exhibit significant luminescent sensitivity to $\text{Cr}_2\text{O}_7^{2-}$ through luminescent quenching effect in aqueous solution, which make its good candidate as luminescent sensor.
$\text{Ag}_2 \cdot \text{CA}$ (CA = cyanuric acid) ⁷	Ag sheets of average Ag-Ag distance around 2.95 Å and hydrogen-bonded CA chains, exhibits anisotropic conductivity and acts as an infinite parallel plate capacitor with a high dielectric constant.

- (1) Wang, H.; Wan, C. Q.; Mak, T. C. W. High-nuclearity silver(I) cluster-based coordination polymers assembled with multidentate oligo- α -heteroarylsulfanyl ligands. *Dalton Trans.*, **2014**, 43, 7254-7262.
- (2) Du, L.-Y.; Shi, W.-J.; Hou, L.; Wang, Y.-Y.; Shi, Q.-Z.; Zhu, Z. Solvent or Temperature Induced Diverse Coordination Polymers of Silver(I) Sulfate and Bipyrazole Systems: Syntheses, Crystal Structures, Luminescence and Sorption Properties. *Inorg. Chem.*, **2013**, 52, 14018-14027.
- (3) Tong, M. L.; Shi, J. X.; Chen, X. M. Photoluminescent two-dimensional coordination polymers constructed with octanuclear silver(I) clusters or silver(I) ions. *New J. Chem.* **2002**, 26, 814-816.
- (4) Xia, C.-K.; Min, Y.-Y.; Yang, K.; Sun, W.; Jiang, D.-L.; Chen, M. Syntheses, Crystal Structures, and properties of Three Novel Silver-organic frameworks Assembled from 1,2,3,5-Benzenetetracarboxylic Acid Based on Argentophilic Interactions. *Cryst. Growth Des.* **2018**, 18, 1978-1986.
- (5) He, Y.; Hu, J.-Y.; Wong, Y.-L.; Diao, Y.; Xian, W.-R. He, J.; Zeller, M.; Xu, Z. Beadwork and Network: Beadwork and Network: Strings of Silver Ions Stich Large- π Pyrazolate Patches into a Two-dimensional Sheet. *Cryst. Growth Des.* **2018**, 18, 3713-3718.
- (6) Jin, J. C.; Jiang, C.; Chang, W. G.; Xu, G. N.; Fu, X. C. A luminescent novel octanuclear silver(I) cluster framework with potential $\text{Cr}_2\text{O}_7^{2-}$ sensing. *Inorg. Chem. Commun.* **2016**, 70, 157-159.
- (7) Rao, C. N. R.; Ranganathan, A.; Pedireddi, V. R.; Raju, A. R. A novel hybrid layer compound containing silver sheets and an organic spacer. *Chem. Commun.* **2000**, 39-40.

(a)



(b)

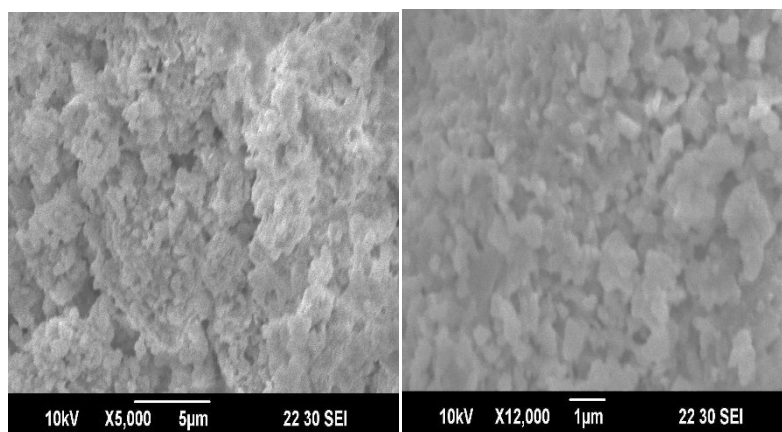


Fig. S1: (a) X-ray powder diffraction ($\text{CuK}\alpha$) pattern of compound I. (b) SEM image of the homogeneous polycrystalline phase synthesized by mechanochemical strategy.

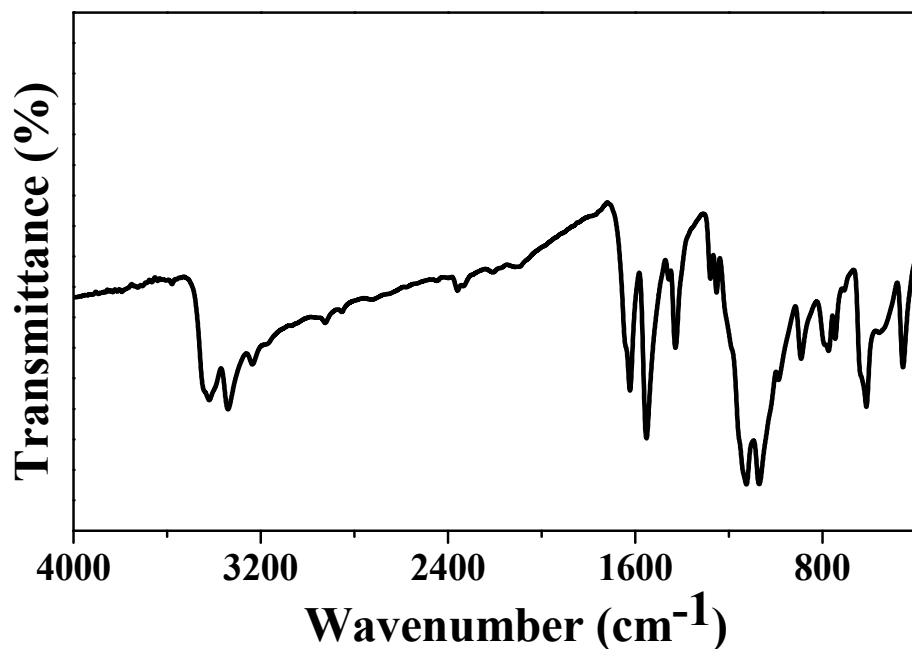


Fig. S2: FTIR Spectrum of compound I.

IR spectrum of the compound is almost similar with earlier reported metal sulfate compounds and can be described concerning five distinct regions. (i) The compound has a sharp doublet band at 3400 – 3320 cm^{-1} region indicative of the presence of the amino group. Doublet band arises due to the symmetric and anti-symmetric stretching of three N-H bonds; (ii) Bands in the region of 1600 – 1430 cm^{-1} are assigned for C-H bending vibrations and due to the asymmetric and symmetric modes of the C-C bond; (iii) 1120 – 1060 cm^{-1} region, with sharp doublet band is due to ν_s (S-O); (iv) The bands are in the region of 880 – 610 cm^{-1} are due to the bending mode of O-S-O of the sulfate unit and (v) the region below 440 cm^{-1} are due to Ag-O stretching frequency. The coordination of sulfate unit to the metal centers decreases the symmetry of the tetrahedral unit, hence the two stretching modes are split in the framework compound. Each sharp peaks contain the shoulders with variable frequencies can be attributed to the bridging coordination of the sulfate unit.

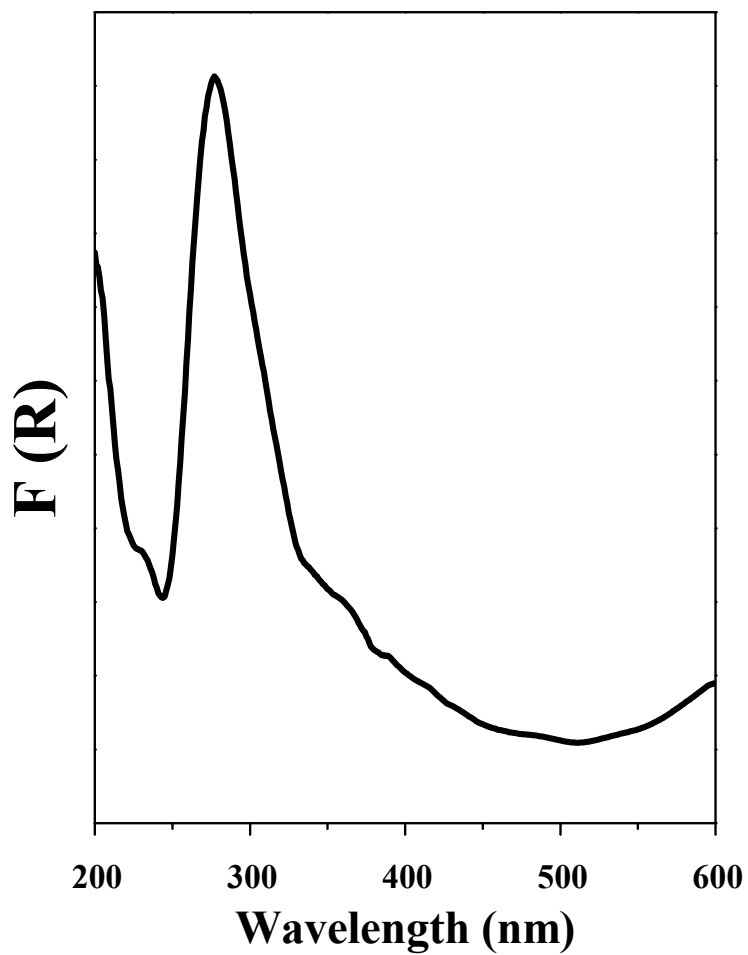


Fig. S3: The diffuse reflectance spectrum of the compound **I** in Kubelka-Munk units. $F(R)$ is the Kubelka-Munk function, where $F(R) = (1-R)^2/2R$, R is the experimentally observed reflectance. There is only one electronic transition at 280 nm which may be the ligand to metal charge transfer (LMCT) for the colorless compound.

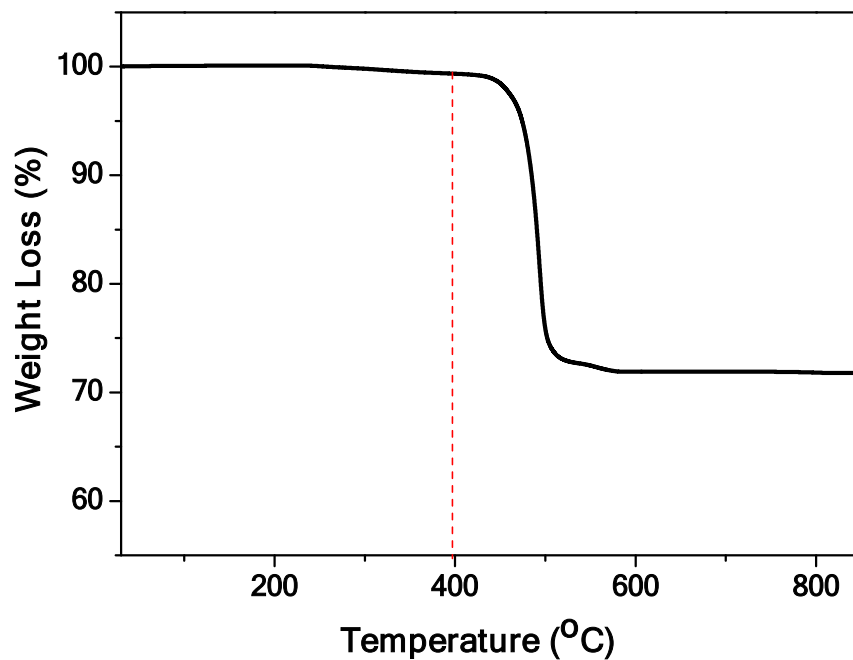


Fig. S4: TGA curve of compound I.

Fig. S4: The studies indicate that the framework is highly stable up to 400 °C. The compound shows weight loss above 400 °C which may be due to the breakdown of the framework structure with the loss of melamine moieties. The total observed weight loss of 27 % appears to match the calculated weight loss (calcd 25 %) due to the loss of organic molecule from the structure. The calcined product was found to be poorly crystalline by PXRD with the majority of the lines correspond to a mixture of Ag_2O and Ag_2SO_4 phases.

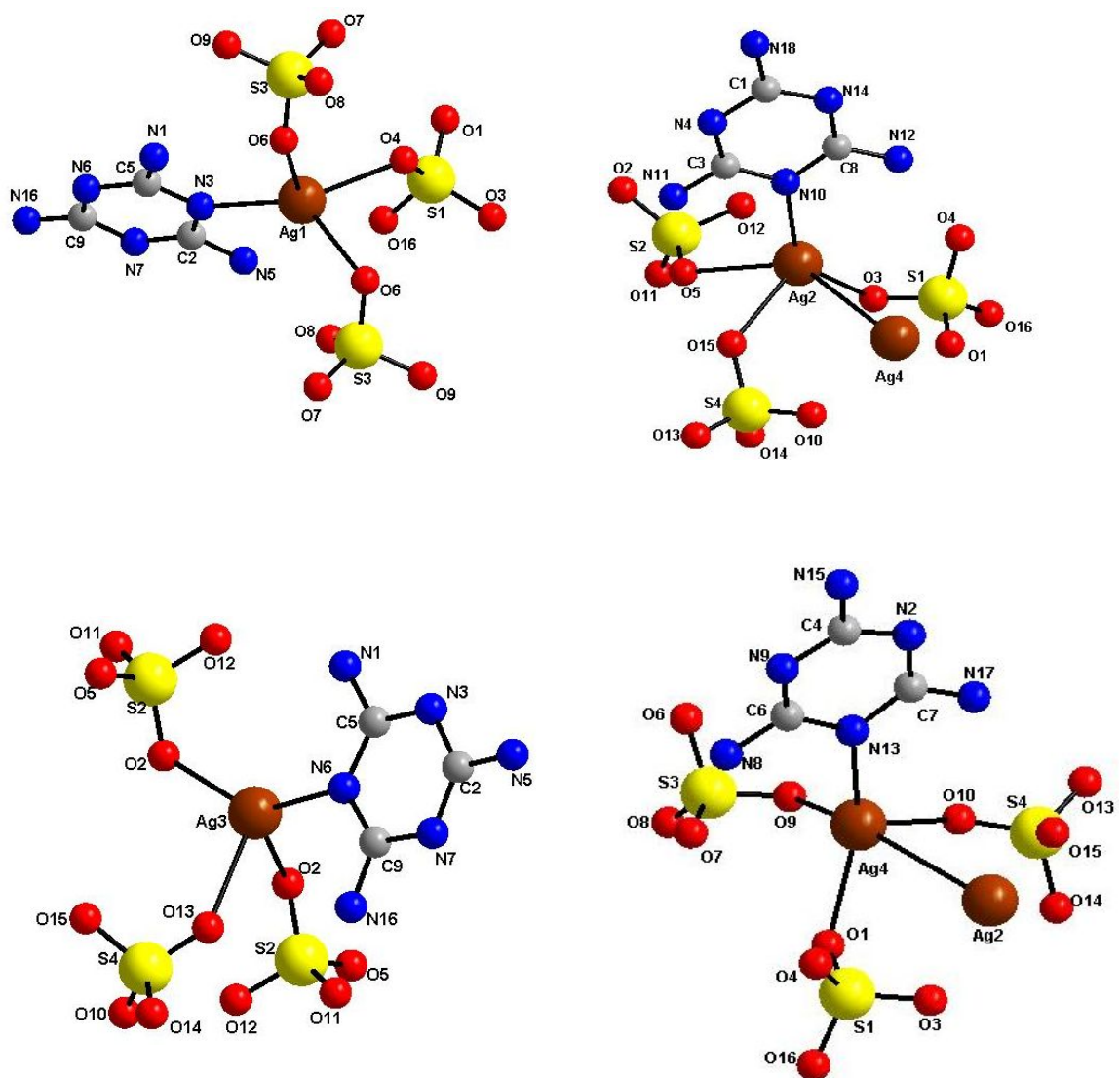


Fig. S5: Coordination environment of the different Silver-ions (Ag1 to Ag4) in the compound I.

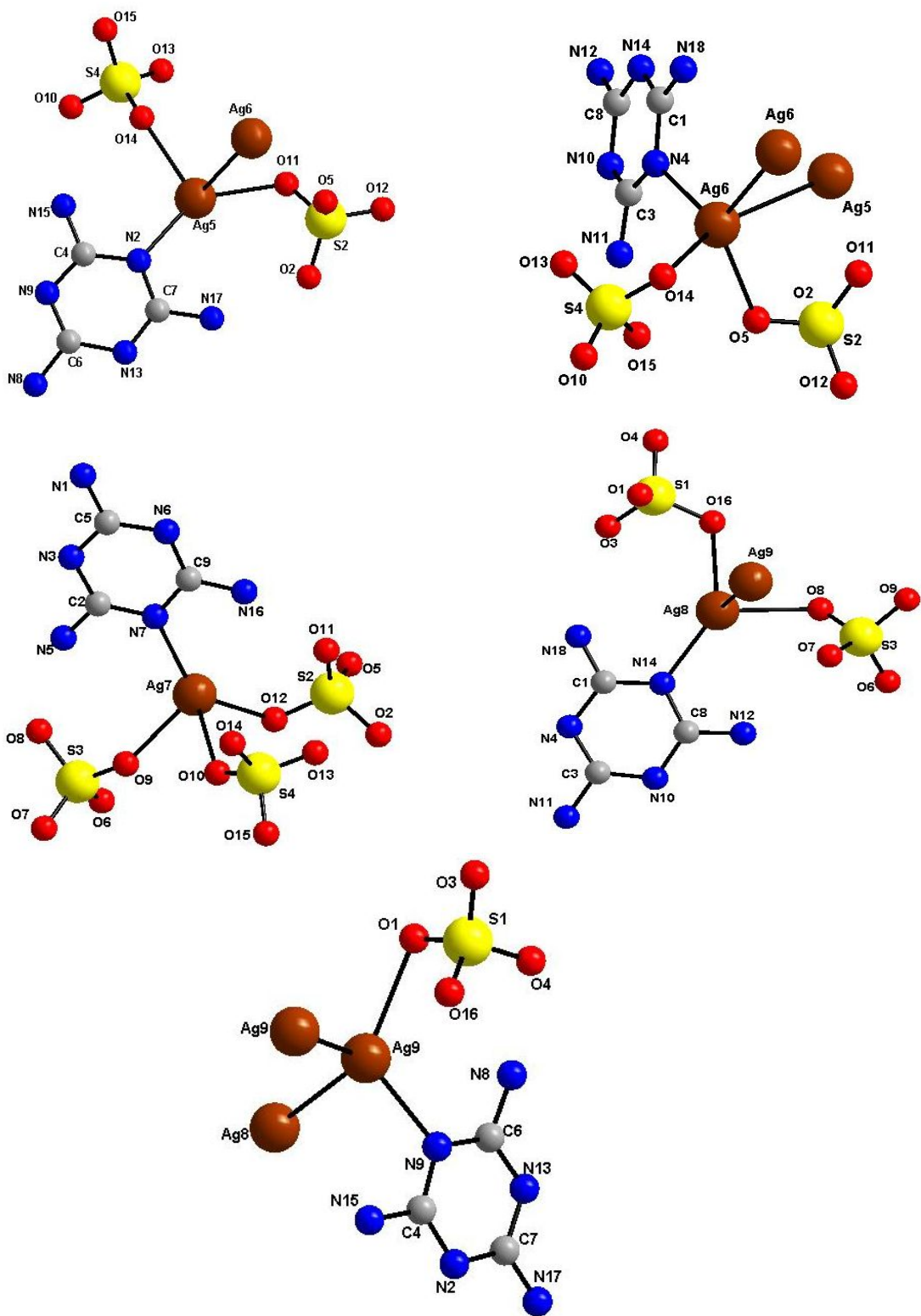


Fig. S6: Coordination environment of the different Silver-ions (Ag5 to Ag9) in the compound I.

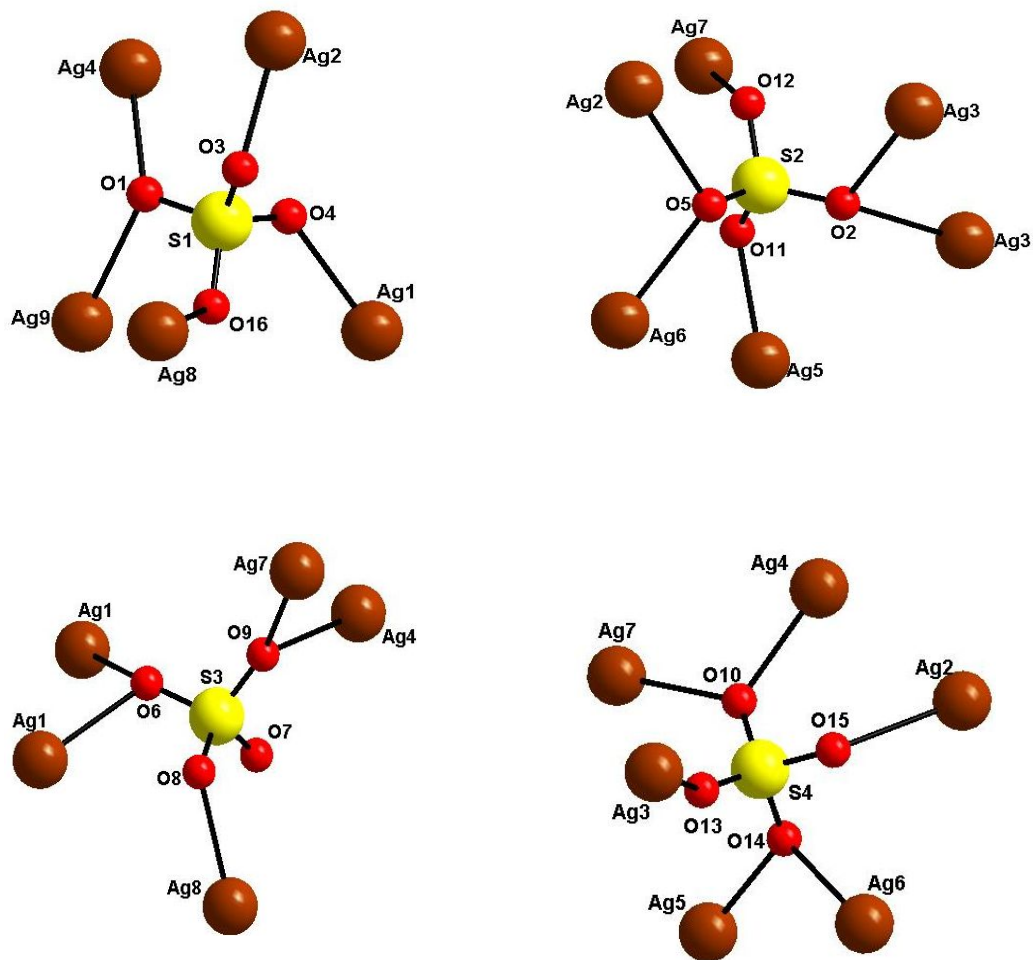


Fig. S7: Coordination environment of the four sulfate units (S1 to S4) in the compound I.

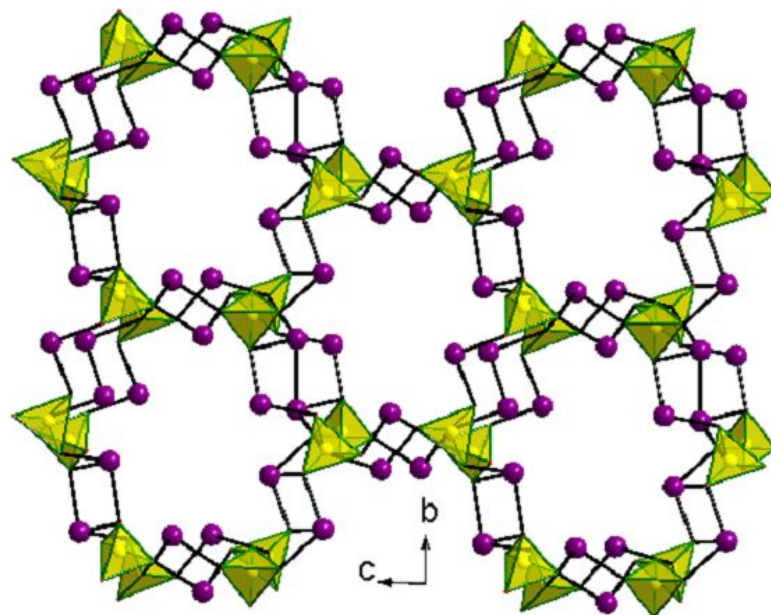


Fig. S8: Figure shows the three-dimensional connectivity of silver ions and sulfate units along *bc* plane. Note that the pores of this structure are occupied by melamine units which cause the damage of the porosity.

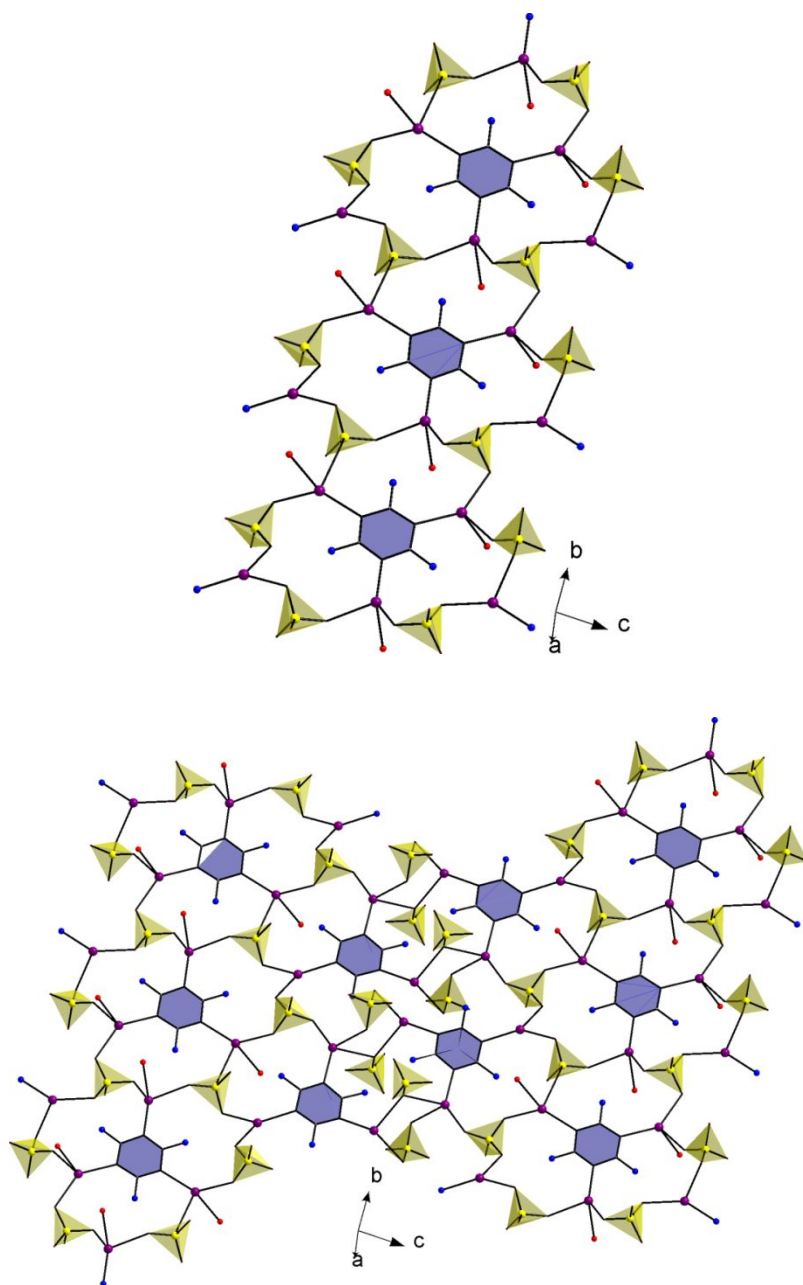


Fig. S9: Figure shows the connectivity of twelve-membered rings forming one-dimensional and two-dimensional arrangements.

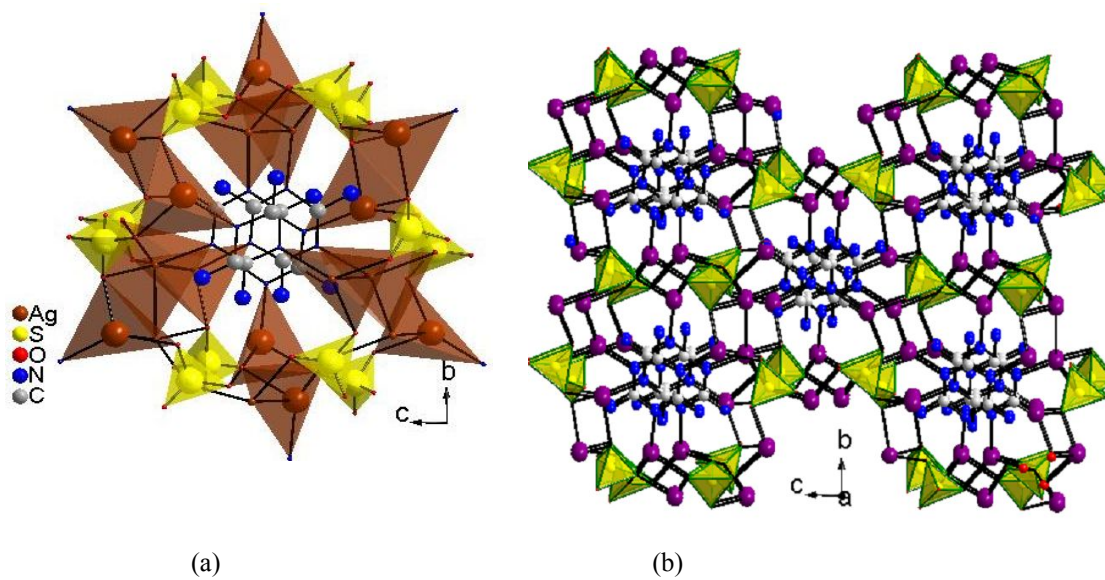


Fig. S10: (a) Figure shows the orientation of melamine units in two-dimensional cluster along the a-axis. (b) Overall three-dimensional connectivity of silver ions, sulfate tetrahedra and melamine units.

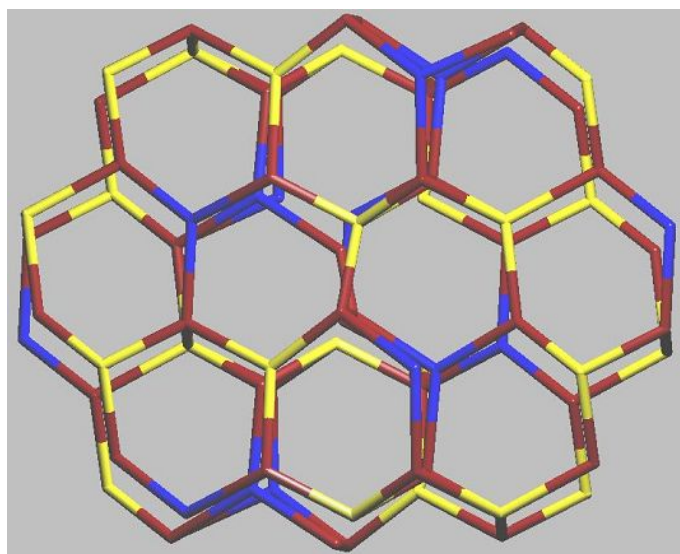
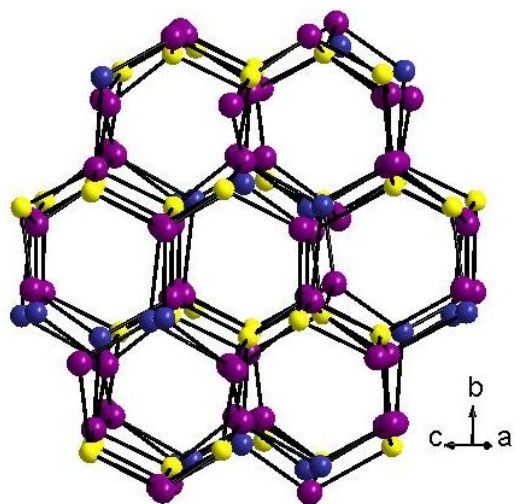


Fig. S11: Topological analysis shows the three-dimensional net observed by node connectivity. Different colors are given for silver-ions (brown), sulfate units (yellow) and melamine units (blue).

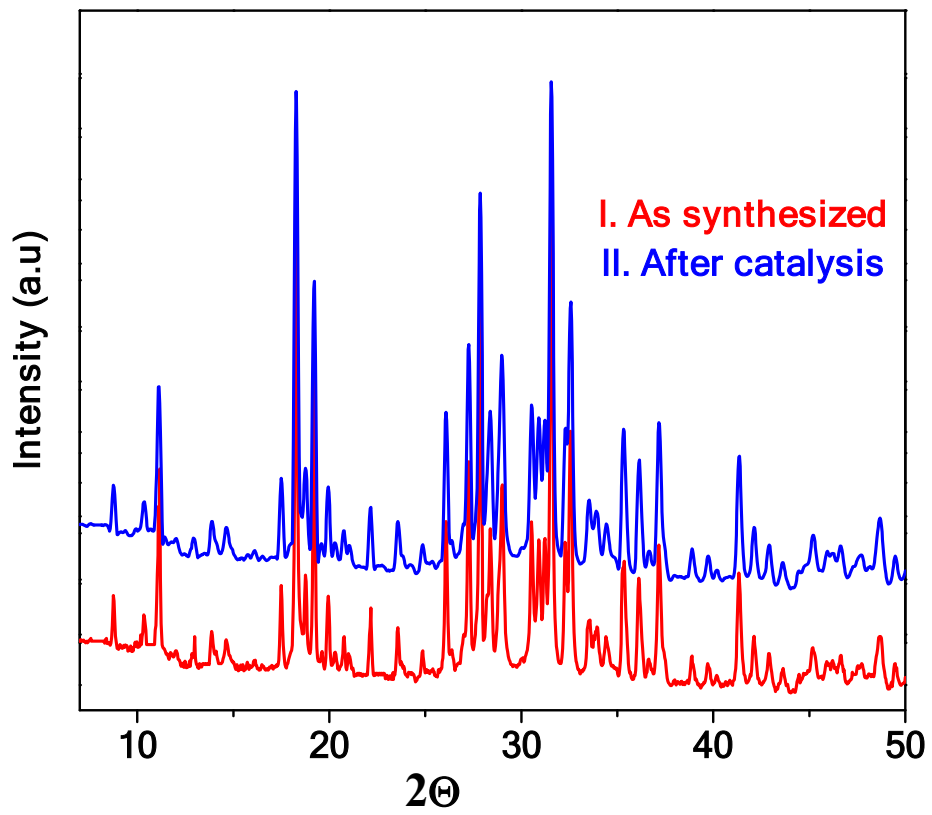


Fig. S12: X-ray powder diffraction ($\text{CuK}\alpha$) patterns of as synthesized compound and compound after catalysis reaction. Only the crystallinity has been reduced a little though there is no structural changes can be observed.

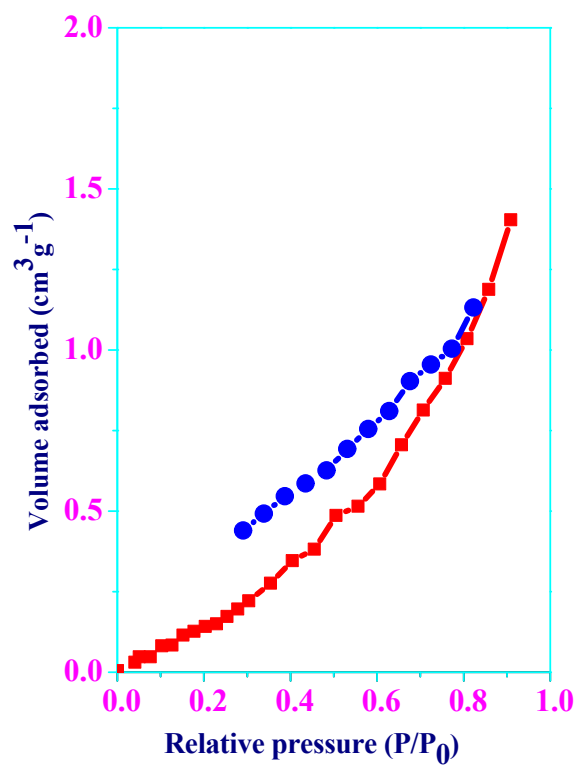


Fig. S13: N₂-gas adsorption and desorption study of the compound **I**. The calculated surface area is 18 m²/g.

Topological Analysis Report

#####

1:C9 N18 Ag8 O16 S4: **Silver ions, sulfate units and melamine units are considered as ZC, ZB and ZA, respectively.**

#####

Topology for ZA1

Atom ZA1 links by bridge ligands and has

Common vertex with R(A-A)

ZC 8 0.7535 0.5962 0.6088 (0 0 0) 3.592A 1

ZC 2 0.6252 1.1368 0.7897 (1 2 1) 3.614A 1

ZC 6 0.5064 0.6378 0.9996 (0 0 0) 3.642A 1

Topology for ZA2

Atom ZA2 links by bridge ligands and has

Common vertex with R(A-A)

ZC 7 0.9662 0.6411 0.2311 (0 0 0) 3.589A 1

ZC 3 1.0645 0.1022 0.0655 (1 0 0) 3.612A 1

ZC 1 0.9138 0.1403 0.4623 (0 0 0) 3.646A 1

Topology for ZA3

Atom ZA3 links by bridge ligands and has

Common vertex with R(A-A)

ZC 5 0.2519 0.6205 0.9106 (0 0 0) 3.611A 1

ZC 4 0.3630 1.1458 0.6924 (1 2 1) 3.617A 1

ZC 9 0.5058 0.6084 0.5234 (0 0 0) 3.657A 1

Topology for ZB1

Atom ZB1 links by bridge ligands and has

Common vertex with R(A-A)

ZC 2 0.3748 0.8632 0.2103 (0 0 0) 3.174A 1

ZC 8 0.2465 0.4038 0.3912 (1 1 1) 3.257A 1

ZC 4 0.6370 0.8542 0.3076 (0 0 0) 3.371A 1

ZC 1 0.0862 0.8597 0.5377 (1 1 1) 3.396A 1

Topology for ZB2

Atom ZB2 links by bridge ligands and has

Common vertex with R(A-A)

ZC 5 0.2519 0.6205 -0.0894 (0 0 -1) 3.178A 1

ZC 7 -0.0338 0.6411 0.2311 (-1 0 0) 3.273A 1

ZC 3 0.0645 1.1022 0.0655 (0 1 0) 3.318A 1

Topology for ZB3

Atom ZB3 links by bridge ligands and has

Common vertex with R(A-A)

ZC 1 1.0862 0.8597 0.5377 (2 1 1) 3.271A 1

ZC 8 0.7535 0.5962 0.6088 (0 0 0) 3.337A 1

ZC 7 0.9662 0.6411 0.2311 (0 0 0) 3.693A 1

ZC 1 0.9138 1.1403 0.4623 (0 1 0) 3.745A 1

Topology for ZB4

Atom ZB4 links by bridge ligands and has

Common vertex with R(A-A)

ZC 4 0.6370 0.8542 0.3076 (0 0 0) 3.449A 1

ZC 5 0.7481 0.3795 0.0894 (1 1 1) 3.515A 1
ZC 2 0.3748 0.8632 0.2103 (0 0 0) 3.551A 1
ZC 7 0.9662 0.6411 0.2311 (0 0 0) 3.559A 1
ZC 3 0.9355 0.8978 -0.0655 (1 1 0) 3.710A 1
Topology for ZC1

c.2

Atom ZC1 links by bridge ligands and has
Common vertex with R(A-A)
ZB 3 1.1519 0.2128 0.5618 (2 1 1) 3.271A 1
ZB 1 0.6698 0.2906 0.6152 (1 1 1) 3.396A 1
ZA 2 0.9881 0.2894 0.2532 (0 0 0) 3.646A 1
ZB 3 0.8481 -0.2128 0.4382 (0-1 0) 3.745A 1
Topology for ZC2

Atom ZC2 links by bridge ligands and has
Common vertex with R(A-A)
ZB 1 0.3302 0.7094 0.3848 (0 0 0) 3.174A 1
ZC 4 0.6370 0.8542 0.3076 (0 0 0) 3.315A 1
ZB 4 0.7096 0.7216 0.1126 (0 0 0) 3.551A 1
ZA 1 0.3409 1.2181 0.2045 (1 2 1) 3.614A 1
Topology for ZC3

Atom ZC3 links by bridge ligands and has
Common vertex with R(A-A)
ZB 2 0.1740 -0.2110 0.0741 (0-1 0) 3.318A 1
ZA 2 -0.0119 0.2894 0.2532 (-1 0 0) 3.612A 1
ZB 4 0.2904 0.2784 -0.1126 (1 1 0) 3.710A 1
Topology for ZC4

Atom ZC4 links by bridge ligands and has
Common vertex with R(A-A)
ZC 2 0.3748 0.8632 0.2103 (0 0 0) 3.315A 1
ZB 1 0.3302 0.7094 0.3848 (0 0 0) 3.371A 1
ZB 4 0.7096 0.7216 0.1126 (0 0 0) 3.449A 1
ZA 3 0.6456 1.2086 0.2883 (1 2 1) 3.617A 1
Topology for ZC5

Atom ZC5 links by bridge ligands and has
Common vertex with R(A-A)
ZB 2 0.1740 0.7890 1.0741 (0 0 1) 3.178A 1
ZC 6 0.5064 0.6378 0.9996 (0 0 0) 3.180A 1
ZB 4 0.2904 0.2784 0.8874 (1 1 1) 3.515A 1
ZA 3 0.3544 0.7914 0.7117 (0 0 0) 3.611A 1
Topology for ZC6

Atom ZC6 links by bridge ligands and has
Common vertex with R(A-A)
ZC 6 0.4936 0.3622 1.0004 (1 1 2) 2.819A 1
ZC 5 0.2519 0.6205 0.9106 (0 0 0) 3.180A 1
ZA 1 0.6591 0.7819 0.7955 (0 0 0) 3.642A 1
Topology for ZC7

Atom ZC7 links by bridge ligands and has

Common vertex with R(A-A)
ZB 2 1.1740 0.7890 0.0741 (1 0 0) 3.273A 1
ZB 4 0.7096 0.7216 0.1126 (0 0 0) 3.559A 1
ZA 2 0.9881 0.2894 0.2532 (0 0 0) 3.589A 1
ZB 3 0.8481 0.7872 0.4382 (0 0 0) 3.693A 1
Topology for ZC8

Atom ZC8 links by bridge ligands and has
Common vertex with R(A-A)
ZC 9 0.5058 0.6084 0.5234 (0 0 0) 3.061A 1
ZB 1 0.6698 0.2906 0.6152 (1 1 1) 3.257A 1
ZB 3 0.8481 0.7872 0.4382 (0 0 0) 3.337A 1
c.3
ZA 1 0.6591 0.7819 0.7955 (0 0 0) 3.592A 1
Topology for ZC9

Atom ZC9 links by bridge ligands and has
Common vertex with R(A-A)
ZC 9 0.4942 0.3916 0.4766 (1 1 1) 2.388A 1
ZC 8 0.7535 0.5962 0.6088 (0 0 0) 3.061A 1
ZA 3 0.3544 0.7914 0.7117 (0 0 0) 3.657A 1
Coordination sequences

ZA1: 1 2 3 4 5 6 7 8 9 10
Num 3 8 16 31 57 74 113 156 199 243
Cum 4 12 28 59 116 190 303 459 658 901

ZA2: 1 2 3 4 5 6 7 8 9 10
Num 3 8 20 37 65 81 122 155 205 260
Cum 4 12 32 69 134 215 337 492 697 957

ZA3: 1 2 3 4 5 6 7 8 9 10
Num 3 8 16 30 53 75 108 153 204 236
Cum 4 12 28 58 111 186 294 447 651 887

ZB1: 1 2 3 4 5 6 7 8 9 10
Num 4 9 19 32 59 86 123 143 203 255
Cum 5 14 33 65 124 210 333 476 679 934

ZB2: 1 2 3 4 5 6 7 8 9 10
Num 3 8 20 34 58 80 118 160 214 247
Cum 4 12 32 66 124 204 322 482 696 943

ZB3: 1 2 3 4 5 6 7 8 9 10
Num 4 11 24 40 70 90 119 159 216 250
Cum 5 16 40 80 150 240 359 518 734 984

ZB4: 1 2 3 4 5 6 7 8 9 10
Num 5 11 21 34 59 93 134 162 211 252
Cum 6 17 38 72 131 224 358 520 731 983

ZC1: 1 2 3 4 5 6 7 8 9 10
Num 4 10 22 46 66 90 118 162 204 276
Cum 5 15 37 83 149 239 357 519 723 999

ZC2: 1 2 3 4 5 6 7 8 9 10
Num 4 8 18 30 54 89 119 167 197 248
Cum 5 13 31 61 115 204 323 490 687 935

ZC3: 1 2 3 4 5 6 7 8 9 10
Num 3 8 18 36 57 89 118 165 204 261
Cum 4 12 30 66 123 212 330 495 699 960

ZC4: 1 2 3 4 5 6 7 8 9 10
Num 4 8 18 31 52 88 119 163 196 249
Cum 5 13 31 62 114 202 321 484 680 929

ZC5: 1 2 3 4 5 6 7 8 9 10
Num 4 10 18 31 58 86 111 171 205 254
Cum 5 15 33 64 122 208 319 490 695 949

c.4
ZC6: 1 2 3 4 5 6 7 8 9 10
Num 3 7 17 30 52 81 113 147 197 256
Cum 4 11 28 58 110 191 304 451 648 904

ZC7: 1 2 3 4 5 6 7 8 9 10
Num 4 11 23 41 57 91 129 159 201 269
Cum 5 16 39 80 137 228 357 516 717 986

ZC8: 1 2 3 4 5 6 7 8 9 10
Num 4 10 19 34 57 91 111 157 197 258
Cum 5 15 34 68 125 216 327 484 681 939

ZC9: 1 2 3 4 5 6 7 8 9 10
Num 3 7 17 29 48 74 113 149 188 234
Cum 4 11 28 57 105 179 292 441 629 863

TD10=941
Vertex symbols for selected sublattice

ZA1 Point symbol: {6^3}
Extended point symbol:[6.6.6(2)]

ZA2 Point symbol: {6^3}
Extended point symbol:[6.6.6]

ZA3 Point symbol: {6^3}
Extended point symbol:[6.6.6(2)]

ZB1 Point symbol: {3.6^2.7^3}
Extended point symbol:[3.6.6.7(2).7(2).7(2)]

ZB2 Point symbol: {6^3}
Extended point symbol:[6.6.6]

ZB3 Point symbol: {4.6^3.8^2}
Extended point symbol:[4.6.6.8(3).6.8(3)]

ZB4 Point symbol: {3.6^2.7^3.8^2.9^2}
Extended point symbol: [3.6.6.7(2).7(2).7(2).8(3).8(3).9.9]

ZC1 Point symbol: {4.6^3.8^2}
Extended point symbol: [4.6.6.8(3).6.8(3)]

ZC2 Point symbol: {3^2.4.6^2.7}
Extended point symbol: [3.6.3.7(3).4.6(2)]

ZC3 Point symbol: {6^3}
Extended point symbol: [6.6.6]

ZC4 Point symbol: {3^2.4.6^2.7}
Extended point symbol: [3.6.3.7(3).4.6(2)]

ZC5 Point symbol: {6^3.7^3}
Extended point symbol: [6.6(2).6.7(2).7.7(2)]

ZC6 Point symbol: {6.10^2}
Extended point symbol: [6(2).10(3).10(3)]

c.5
ZC7 Point symbol: {6^3.8^3}
Extended point symbol: [6.8.6.8(2).6.8(3)]

ZC8 Point symbol: {6^3.7^3}
Extended point symbol: [6.6(2).6.7(2).7.7(2)]

ZC9 Point symbol: {6.8^2}
Extended point symbol: [6(2).8.8]

Point symbol for net:
{3.6^2.7^3.8^2.9^2} {3.6^2.7^3} {3^2.4.6^2.7} 2 {4.6^3.8^2} 2 {6.10^2} {6.8^2} {6^3.7^3} 2 {6^3.8^3} {6^3} 5
3,3,3,3,3,3,4,4,4,4,4,4,4,4,5-c net with stoichiometry (3-c)(3-c)(3-c)(3-c)(3-c)(3-c)(4-c)(4-c)(4-c)(4-c)(4-c)(4-c)(4-c)(5-c); 16-nodal net

New topology, please, contact the authors (17467 types in 3 databases)

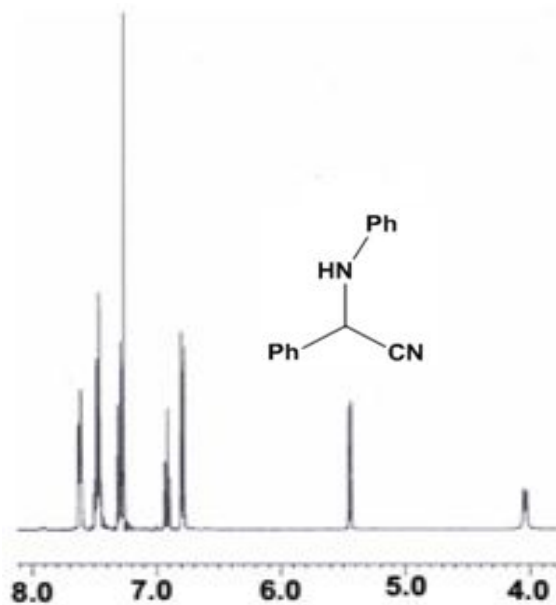
Elapsed time: 34.95 sec.

Ref.

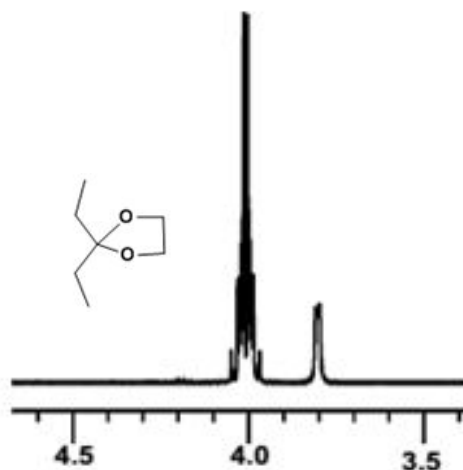
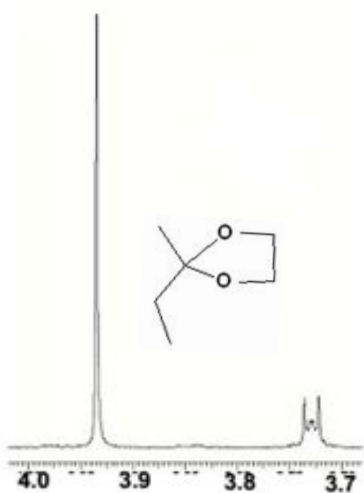
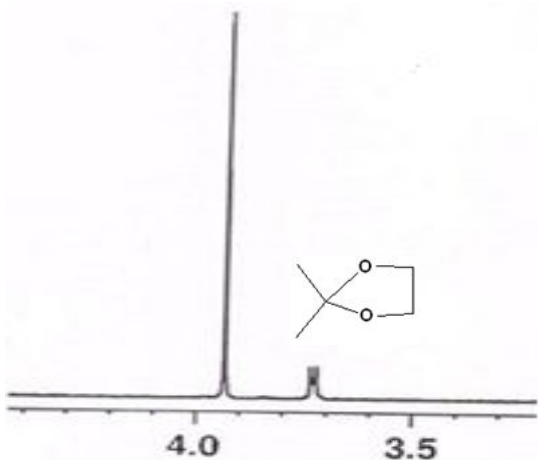
- (1) V. A. Blatov, A. P. Shevchenko, Latest version 2017, www.topospro.com ;
- (2) V. A. Blatov, A. P. Shevchenko, D. M. Proserpio, *Cryst. Growth Des.* 2014, **14**, 3576;
- (3) V. A. Blatov, M. O'Keeffe, D. M. Proserpio, *CrystEngComm*, 2010, **12**, 44.

Catalytic Reactions:

Cyanosilylation Reaction: In a typical experiment, powdered catalyst (35 mg, 0.02 mmol) was suspended in 100 ml round bottom flask with the CH_2Cl_2 solvent (50 mL) and N-benzilidine aniline (0.36 g, 2 mmol). Trimethylsilyl cyanide (0.30 g, 3 mmol) was added to it at 0 °C and the overall mixture was stirred for 2 h in N_2 atmosphere. The product was filtered through Millipore membrane filter papers to remove the catalyst particles. The supernatant liquid was dried under vacuum to remove the solvent. The product was analyzed and evaluated for the conversion of the reactants through ^1H NMR spectra.



Ketalization Reaction: We used three different ketones i.e. acetone, 2-butanone and 3-pentanone. Typically, 0.02 mmol (35 mg) portion of the silver sulfate catalyst, 16 mmol of acetone (0.92 g), and 16 mmol of ethylene glycol (0.99 g) were introduced into 10 mL of toluene, the latter was used as the solvent for a ketal formation reaction. The reaction was refluxed at 60 °C for 10 h. After completion of the reaction, the catalyst was isolated by filtration and reused on subsequent reactions without further treatment.



Esterification Reaction: we carried out the esterification between acetic acid and ethanol with silver sulfate catalyst. 0.02 mmol (35 mg) catalyst, 16 mmol of acetic acid (0.96 g), and 16 mmol of ethanol (0.74 g) were introduced into 10 mL of toluene for this catalytic reaction. Catalyst and substrate ratio was 1:800 similar to the ketalization.

